SINERGI Vol. 26, No. 3, June 2022: 295-302
http://publikasi.mercubuana.ac.id/index.php/sinergi
http://doi.org/10.22441/sinergi.2022.3.004

Analysis of variance dimension of reinforcement to stress concentration factor using Finite Element Method

Ali[1], Diki Ismail Permana[1,2*], Hermawan Nurfakhriza Yudha[1]
[1]Department of Mechanical Engineering, Faculty of Industrial Engineering, Institut Teknologi Nasional Bandung, Indonesia
[2]Doctoral Study of Mechanical Engineering, Hungarian University of Agriculture and Life Science, Hungary

Abstract
Stress concentration is a condition when stress increases only at a certain area of a component compared to the stress at the uniform cross-section of the component when given a load. This phenomenon can occur due to irregular geometry such as a hole, sharp angle, cross-section change, notch, threads, groove, crack, etc. Any change in geometric shape on a uniform cross-section will cause a stress increase. Therefore, high-stress concentrations need to be reduced to prevent the faster failure of a component. The stress concentration can be determined using stress concentration factors (K_t). Using the Finite Element Method (FEM) method, the simulation obtained stress distribution in the modelled shaft without and with the additional groove. The results obtained by adding a semi-circular groove can reduce stress concentrations by up to ten percent.

Keywords:
Fatigue;
Finite Element Method;
Notch;
Release stress groove;
Simulation;

Article History:
Received: December 10, 2021
Revised: February 14, 2022
Accepted: February 20, 2022
Published: October 4, 2022

Corresponding Author:
Diki Ismail Permana, Mechanical Engineering Department, Institut Teknologi Nasional Bandung, Indonesia, Doctoral Study of Mechanical Engineering, Hungarian University of Agriculture and Life Science, Hungary
Email: dicky91permana@itenas.ac.id

INTRODUCTION

Stress concentration is a condition when the stress increases only in a certain area of a component compared to the stress in the uniform part of the component when it is given a load. This phenomenon can occur due to geometric irregularities such as holes, sharp angles, changes in cross-section, notches, threads, grooves, cracks, and so on [1][2]. Any change in geometric shape in a uniform cross-section will cause an increase in stress. The location of stress concentration usually occurs around the irregular geometry area. The high-stress concentrations need to be reduced to prevent faster failure of a component. For example, cracks that occur begin in the stress concentration region. The value of the stress concentration that happens can be known by using the stress concentration factor (K_t).

However, the machine's components do not always have a uniform cross-section. For example, a shaft has two different diameter sizes equipped with fillets, so the stress concentration occurs in the fillet section. The way that can be done to reduce stress concentration is to provide additional grooves on these components. The extra track will be a reinforcement because it helps distribute the stress in the stress concentration area so that the stress that occurs in that area becomes smaller. The reduction's magnitude depends on the reinforcement grooves' size and location in the stress concentration region.

Additional grooves in a shaft can be stated to be a relatively simple approach to reduce stress concentrations and extend shaft fatigue life, provided the suitable size and location of groove positions are chosen. The effectiveness of using more grooves has been demonstrated by experience and theoretical analyses (stress reduction) [3]. The reduction of stress concentration using an additional groove was first proposed by Peterson [2]. It was found that adding grooves could reduce the stress concentration, which was experimentally proven by Ermishkin et al. [4]. The study determination of stress concentration factors using photometric analysis

stated that adding a notch to Aluminium alloy decreases the cross-section moment resistance.

Analyzing the effect of the reinforcing groove's size and location on stress concentration reduction requires a lot of experimentation. Some ways that can be used to save the cost and time of the experiment is by modelling analysis using ANSYS software. The purpose of this study is to get the relationship between the additional of the plot reinforcement to the stress concentration factor value (K_t), make a graph of the factor stress concentration (K_t) from the analysis using ANSYS software, and know the stress concentration reduction that occurs in the modelling. On the other hand, Muminovic et al. [5] only study a concentration factor on the shaft using CATIA along the cut area surface. Furthermore, Liang et al. [6] conducted an experimental investigation of artificial pitting on the stress concentration factor of the mechanical properties of steel plates.

Moreover, Ozkan and Toktas [7] studied a determination of the stress concentration factor in a rectangular hole under tensile stress using different methods. The best way to obtain the results is using an Artificial Neural Network (ANN) method compared to FEA. Meanwhile, Norton [8] proposed making design changes such as relief grooves to qualitatively lower stress concentrations in step shafts without providing quantitative data on the groove geometry.

The application of reducing stress concentration with the addition of a notch has also been applied to gears. Vuckovic et al. [9] predicted the bending fatigue failure using numerical simulation with adding a dimension and shape to the adjacent tooth. Kumar et al. [10] carried out numerical research on gears to reduce stress in the root fillet region. Furthermore, Sutar et al. [11] summarize the papers contains the effect of relief stress grove on gears and improved the placement of these elements to reduce stresses and extend the life of the gear.

. Therefore, they ran various experiments with varying numbers of features and feature combinations. Therefore, this study provides an exact dimension of the addition reinforcement grooves through modelling and analysis of the reduction of stress concentration in the modelling result.

METHOD

Dimension of Shaft without Reinforcement

Initial calculations are carried out to obtain the normal stress and maximum stress on the shaft modelling with two-fillet diameters with axial load in the form of tensile load. The maximum normal stress value can be obtained by multiplying the nominal normal stress with the stress concentration factor (K_t) obtained from Figure 1 and stated as: (1), (2) and (3) [12].

$$\sigma_{normal} = \frac{F}{A} \quad (1)$$

$$\sigma_{max} = \frac{M.C}{I} \quad (2)$$

$$K_t = \frac{\sigma_{max}}{\sigma_{normal}} \quad (3)$$

Where A is the cross-sectional area (m^2), F is the force (N), M is the moment (N.m), C is the distance from the centre of the object to the target point (m), I is the inertia (m^4), and σ_{normal}, σ_{max} is the normal stress and maximum stress (Pa), respectively.

The shaft model is made with the geometry as shown in Figure 2. The shaft is made of stainless steel with a modulus of elasticity (E) 193 GPa, and a poison ratio of 0.31. The shaft is given an axial load of 100 N with a concentrated load while the other side is clamped. For initial calculation, the authors set the shaft geometry with the ratio of D/d = 2.

Therefore, the initial value of the dimensions used in this study for the large diameter (D) is 150 mm, and the small diameter (d) is 75 mm. Next, the normal stress value is obtained by using (1), the value of σ_{normal} is 22635.37 Pa.

Based on the initial data that has been known, namely D/d = 2 and r/d = 0.3, then to determine the stress concentration factor, then plot the data. Draw a straight line from r/d = 0.3 until it meets the gradient D/d = 2, then form a right angle from the initial line formed and direct it towards K_t.

From Figure 2, plotted, the stress concentration factor value is 1.48, so the maximum stress obtained using (3) is 33345.7 Pa.

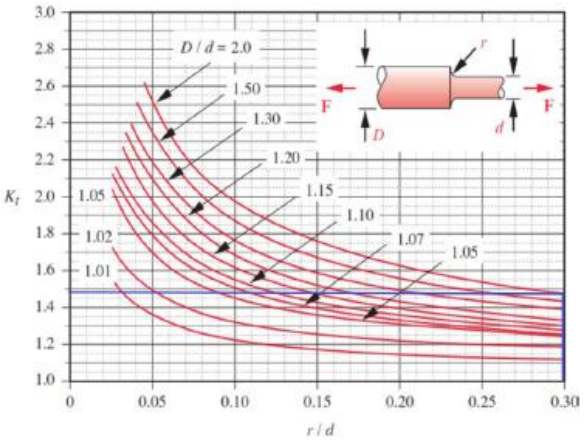

Figure 1. The factor of stress concentration (K_t) [13]

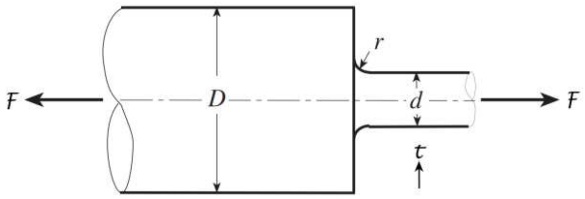

Figure 2. Modelling shaft [14]

Dimension of Reinforcement on Shaft

This section discusses the size of the shaft that is being modelled. The discussion starts from the fillet size and the reinforcement's radius to the size the distance between the reinforcement. Figure 3 shows the shaft dimension with reinforcement, where:

D: large diameter (mm)
d: small diameter (mm)
r: fillet (mm)
t: the difference between D and d of the shaft (mm)
L1: the distance to the radius of R1 (mm)
L2: the distance between R1 and R2 (mm)
R1: radius of reinforcement groove 1
R2: radius of reinforcement groove 2

According to the figure, the authors use ISO 18388:2016, specifying a series of relief grooves for shafts and holes for general use in mechanical engineering.

Furthermore, Table 1 and Table 2 are dimension variations of the first reinforcement groove (R1), smaller than the filet dimensions, so that the stress concentration grooves can be evenly distributed. Similarly, with reinforcement groove (R2), the magnitude is the same and smaller than R1, so it gets the effect of reducing the voltage concentration.

Simulation Setup

In this study, several settings were applied to achieve good simulation results; namely, the type of stainless steel material selection when setting engineering data on ANSYS is provided in Table 3. The basic settings applied to meshing are to set the physics preference to mechanical, element order to quadratic, and the method used is tetrahedrons.

Then the sizing section changed its resolution to 2, smoothing to medium, and span angle to fine.

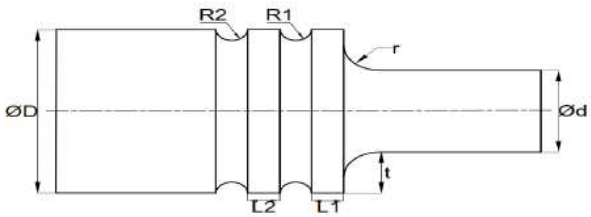

Figure 3. Shaft dimension with reinforcement

Table 1. Variation of fillet dimension

r/d	0.05	0.075	0.1	0.125	0.15	
	0.175	0.2	0.25	0.275	0.3	
r (mm)	3.75	5.625	7.5	9.375	11.25	13.12
	15	16.87	18.75	20.62	22.5	

Table 2. Variation of reinforcement dimension

No of reinforcement	D (mm)	d (mm)	L1 (mm)	R1 (mm)	L2 (mm)	R2 (mm)
1	150	75	20	25	20	25
2	150	75	20	25	20	22,5
3	150	75	20	25	20	20
4	150	75	20	25	20	17,5
5	150	75	20	25	20	15
6	150	75	20	25	20	12,5
7	150	75	20	25	20	10
8	150	75	20	15	20	15
9	150	75	20	15	20	12,5
10	150	75	20	15	20	10
11	150	75	20	30	20	30
12	150	75	20	20	20	20
13	150	75	20	10	20	10

Table 3. Stainless steel material properties [15]

Properties	Value	Units
Density	7600-8100	$Kg.m^{-3}$
Coefficient of Thermal expansion	1.7×10^{-5}	C^{-1}
Young's Modulus	$19 – 20 \times 10^{11}$	Pa
Poisson's Ratio	0.31	
Bulk Modulus	1.693×10^{11}	Pa
Shear Modulus	7.366×10^{10}	Pa
Tensile Yield Strength	$4.8 – 22x\ 10^{8}$	Pa
Compressive Yield Strength	2.07×10^{8}	Pa
Tensile Ultimate Strength	$4.8 - 22 \times 10^{8}$	Pa
Strength exponent	-0.15	
Ductility exponent	0.55	
Cycling strength coefficient	1.96×10^{9}	Pa
Specific heat (1350 °C)	450 – 530	J/kg.°C
Energy	80 - 89	MJ/kg

Meshing settings are needed to overcome the limitations imposed by the software due to the use of student licenses and increase the accuracy of simulation results. The resulting nodes are about 20000 nodes using the settings as above. The next step is to determine the type of support and the type of loading, and its value to be used in the shaft simulation. This arrangement can be made on the static structural part. In this study, the type of support used is a *fixed joint* which is applied to the surface of the large shaft and the force of 100 Newton to the surface of the small shaft is applied in the direction of the x component.

Figure 4 shows the simulation on the axis that has been modelled. The results are that the nominal normal stress is 22635 Pa and the maximum normal stress is 33707 Pa. While Figure 5 is the simulation on the axis that has been modelled, the results obtained are nominal normal stress 22635 Pa and maximum normal stress 33052 Pa.

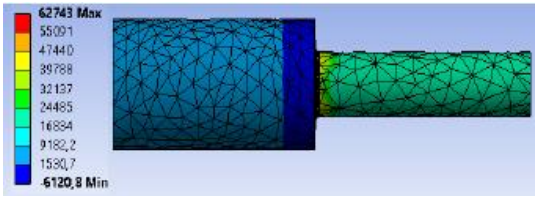

Figure 4. Shaft without reinforcement

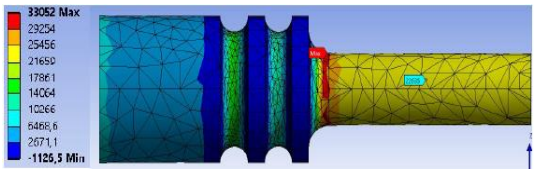

Figure 5. Shaft with reinforcement

This early stage research intends to observe the software's ability to show the nominal normal voltage results. Theoretically, the nominal normal stress results in calculations, modelling without reinforcement, and modelling with reinforcement must be the same because the size of the radius of the reinforcement used does not exceed the difference between the large diameter and the small diameter shaft.

RESULTS AND DISCUSSION

The Effect of Reinforcement on Stress Concentration

The simulation results show a phenomenon, the addition of a reinforcement groove can reduce the stress concentration. However, it was also found that there were variations in the size of certain reinforcement grooves, which caused the decrease in stress concentration. In general, it can be stated that the addition of reinforcing grooves can reduce the stress concentration factor (K_t).

Figure 6 shows the effect of the stress concentration factor (K_t) with the variation of reinforcement (R2) with constant R1 (25 mm). This reinforcement size variation aims to observe the maximum normal stress for the shaft, which has the first reinforcement size approaching the shaft fillet. It can be seen in the figure of r/d at 0.075 that the shaft with $R2_3$ = 20 mm produces the smallest stress concentration with 11.6% reduction, followed by the shaft with $R2_6$ = 12.5 mm, $R2_2$ = 22,5 mm, $R2_5$ = 15 mm, $R2_4$ = 17.5 mm, and shaft without reinforcement produces the highest stress concentration. Figure 7 shows the effect of the stress concentration factor (K_t) with the variation of reinforcement (R2) with constant R1 (15 mm).

The application of this reinforcement size variation aims to observe the maximum normal stress for the shaft with the first reinforcement size away from the shaft fillet direction. It can be seen in the figure of r/d at 0.125 that the shaft with $R2_9$ = 12.5 mm produces the smallest stress concentration with a 7.93% of reduction, followed by the shaft with $R2_{10}$ = 10 mm, $R2_8$ = 15 mm, and the shaft without reinforcement produces the highest stress concentration. Figure 8 shows the effect of stress concentration factor (K_t) with R1 = R2. The application of this reinforcement size variation aims to observe the maximum normal stress for the shaft if the size of the first reinforcement and the second amplifier is the same. It can be seen that r/d at 0.125 that the shaft with $R2_{11}$ = 30 mm produces the smallest stress concentration with a 10.33% of reduction, followed by the shaft with $R2_{12}$ = 20 mm, $R2_{13}$ = 10 mm.

The tendency for improvement, nonetheless, was not monotonic. For example, it can be seen in Table 4 for R1 = 25 mm, where the best r/d value is 0.075, while the best R2 value is at 20 mm with an 11.60% reduction. The smaller value of R2 and the smaller percentage of reduction can be seen, but there is a limit to the maximum of R2. It is due to the location of the maximum stress, which can fail the shaft in the contact area, which is transmitted to the area where there is a reinforcing groove so that the maximum stress on the leading edge can be reduced. Figure 10 shows the result of the reinforcement groove that spreads the maximum stress and reduces the failure of the shaft compared to the shaft without the reinforcement groove shown in Figure 9.

Similar results were also proved by Erena et al. [16], who investigated the influence of artificial internal stress relief groove in fretting fatigue and by Onyegiri et al. [17], that optimized the threaded connectors for sandwich pipe using stress relief groove. Zeng et al. [18] also suggested a finite element (FE) model to simulate fretting wear and fatigue in press-fitted railway axles. The results suggest that increasing groove depth or decreasing groove radius can reduce fretting wear and improve fretting fatigue strength by reducing stress concentration.

Table 4. Simulation result of reinforcement groove combinations

R1 (mm)	R2 (mm)	r/d	σ_{max} (N.m^2)	K_t	Reduction (%)
25	25	0.075	49551	2.19	10.38
25	22,5	0.075	49176	2.17	11.07
25	20	0.075	48876	2.16	11.60
25	17,5	0.075	49528	2.19	10.42
25	15	0.075	49493	2.19	10.48
25	12,5	0.075	49037	2.17	11.31
25	10	0.075	49734	2.20	10.05
15	15	0.125	43095	1.90	6.50
15	12,5	0.125	42623	1.88	7.53
15	10	0.125	42907	1.89	6.91
30	30	0.05	56426	2.49	10.07
20	20	0.05	57839	2.55	7.82
10	10	0.05	59026	2.61	5.92

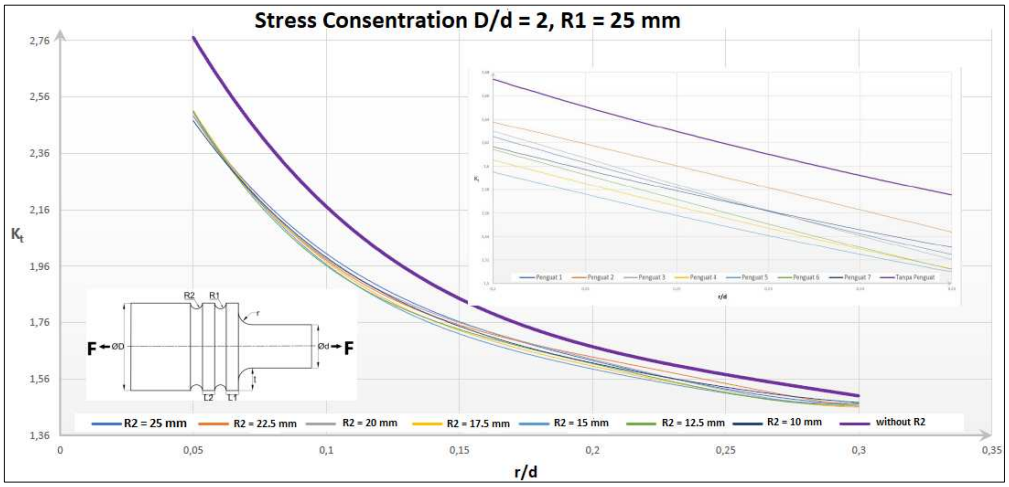

Figure 6. Stress concentration factor (D/d = 2, R1 = 25 mm)

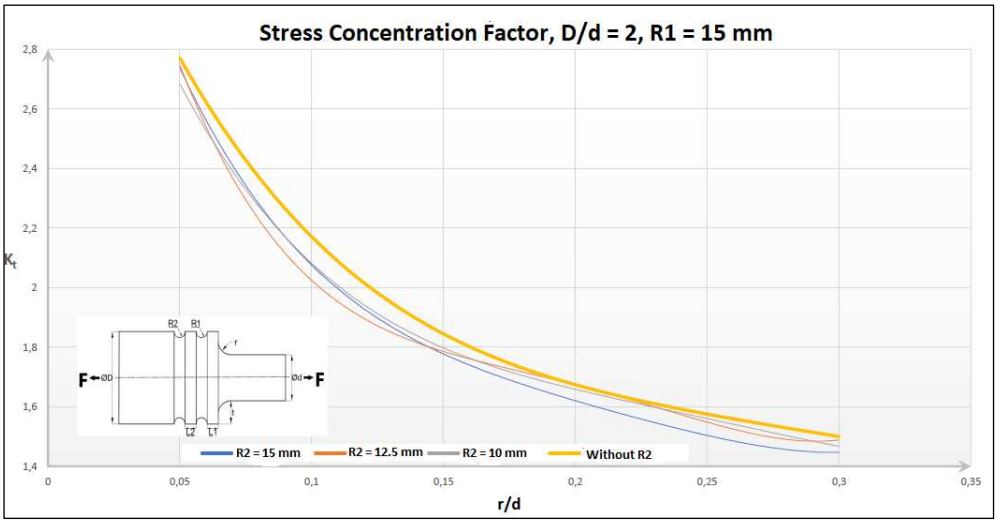

Figure 7. Stress concentration factor of (D/d = 2, R1 = 15 mm)

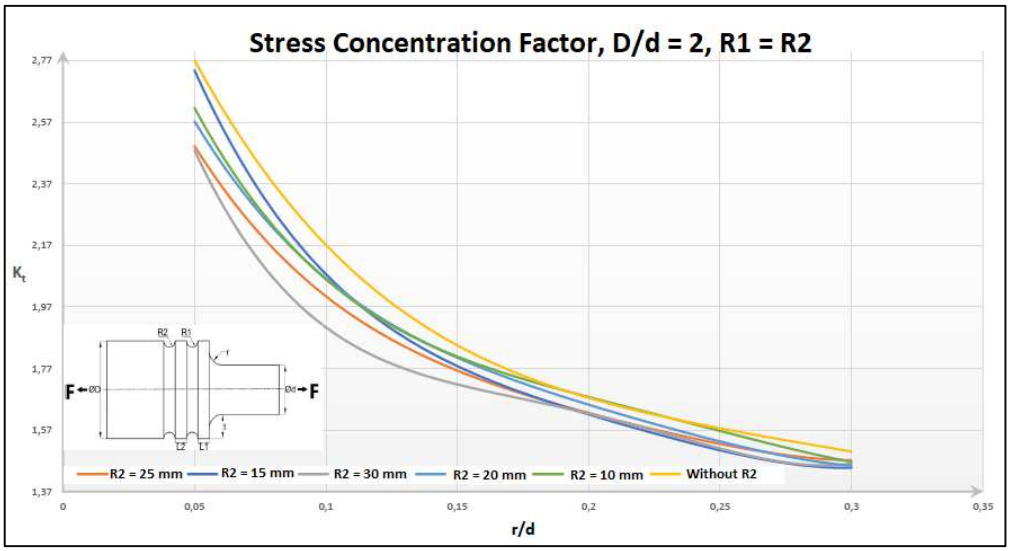

Figure 8. Stress concentration factor of (D/d = 2, R1 = R2)

Result of Stress Distribution

FEM analysis determines the nominal normal stress and the maximum normal stress that occurs in the simulated multilevel shaft. It can also be used to determine the stress distribution that occurs [19][20]. The stress distribution that occurs can be observed by performing a cross-section on the shaft, which has been simulated. Simulation results are listed for shafts with r/d = 0.2 or 15 mm fillet size and for different sizes of reinforcement. Observation of stress distribution was carried out to see the influence of the size variation of the reinforcement used to distribute the stress to reduce the stress concentration in the fillet section. After observing the behavior of the reinforcement groove variation in reducing stress concentration, the dimensions of the reinforcing groove that are best in reducing stress concentration will be obtained.

It can be observed that the stress concentration continues to occur in the fillet section for the gradual shaft without reinforcing grooves and for graded shafts with reinforcing grooves. Even so, it can be seen that the stress distribution occurs very different, where the multilevel shaft with reinforcing grooves has a more even distribution of stress. The stress that occurs is not only concentrated in the fillet area but is evenly distributed towards the large diameter part of the shaft.

It can be seen in Figure 9 and Figure 10 that there is a reduction in the maximum stress concentration as significant as 2109 Pa in the notch area in the shaft, which has reinforcement dimensions R1 = 25 mm, R2 = 15 mm. Moreover, Figure 11, Figure 12, and Figure 13 are the shaft with the addition of two reinforcements of the same size of 10 mm, 20 mm and 30 mm, respectively. Moreover, it can be seen in Figure 11-12 that there is a decrease in maximum stress concentration with the increase in dimensions of the reinforcement. This is evidenced by a wider area of color gradation on the shaft with a large reinforcing groove. In this case shaft with R1=R2=30 mm produces the smallest maximum stress concentration with 36589 Pa, followed by a shaft with R1=R2=20 mm and R1=R2=10 mm with 36659 Pa and 37784 Pa, respectively.

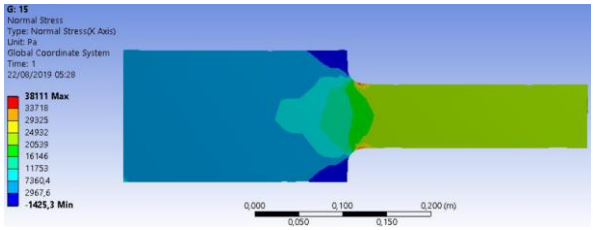

Figure 9. Shaft without reinforcement

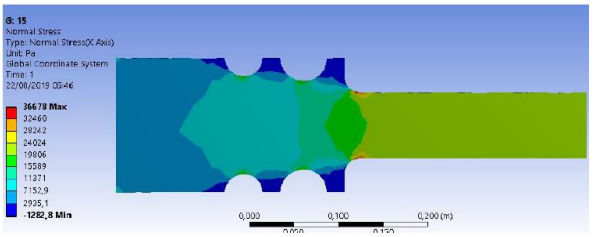

Figure 10. Shaft with R1=25 mm, R2=20 mm

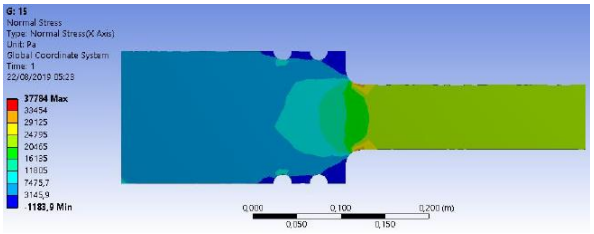

Figure 11. Shaft with R1= R2 = 10 mm

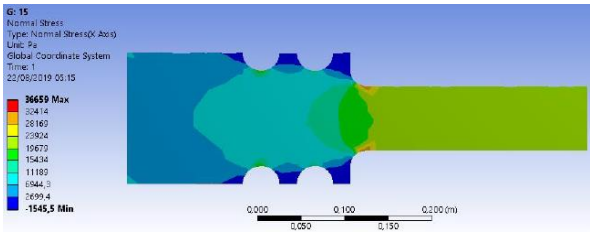

Figure 12. Shaft with R1 = R2 = 20 mm

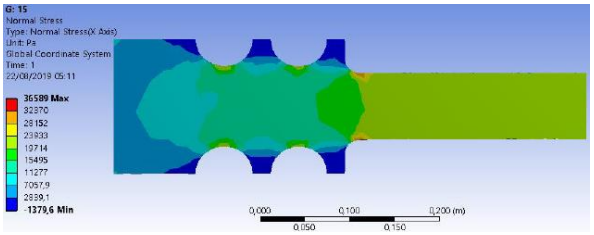

Figure 13. Shaft with R1 = R3 = 30 mm

In addition, the results of the stress distribution from the ANSYS simulation obtained different behavior between the reinforcement grooves, which have the same size and the amplifier grooves, which have different sizes of R1 and R2. When Figure 9, Figure 10, Figure 11, and Figure 12 are observed, when the sizes between reinforcement R1 and R2 are made different, it can be seen that there is a considerable impact in distributing the stress concentration. As shown in Figure 9, when the difference in the size of the shaft geometry gets gentler, the stress distribution is better. It can also be seen from the maximum normal stress that occurs at the lowest value with the widest area of color gradation. Thus, the reinforcing groove can reduce the stress concentration in the fillet part of the shaft even though the value is not uniform.

Similar results research by Mantovani et al. [21] proposed a simplified method for evaluation

of multiaxial stress concentration factors (SCFs) to account the poisson's ratio effect for U-grooved shafts. Moreover, Wang et al. [22] conduct a simulation and an experimental investigation on elasto-hydrodynamic lubrication of the journal bearing system using a relief groove in the scroll compressor.

In experimental investigation, Ma et al. [23] researched the effect of fitting morphologies on the static behavior of steel bars with the addition of notch variation, and H. Zeng et al. [24] predicted notch wear of AerMet100 to influence stress concentration. Both of the research resulted in the similar characteristic of addition notch or reinforcement will decrease stress concentration at some level. Furthermore, Zhu et al. and Asmara [25][26] compiled some researches of notch effects in metal fatigue, and they concluded that the influence of notch effect on fatigue lifetime reduction is a barrier that cannot be avoided in structural design of engineering components. Only by precisely understanding the effect of notch features on fatigue strength can theoretical approaches consistent with fatigue failure mechanisms be devised, avoiding conservative design and reaching optimal structure design. As a result, the works mentioned earlier in the literature are intended to strengthen the findings of this study about shaft reinforcement in response to stress concentration.

CONCLUSION

Adding reinforcing grooves, in general, can reduce the stress concentration that occurs in an object to reduce the risk of failure of the object when given a load. The reinforcement groove aims to refine the stress distribution that occurs. The reinforcing groove indirectly distributes the stress to the narrowed part of the object. It can be concluded based on the analysis that the shaft with reinforcement R1=25mm and R2=15mm produces the smallest σ_{max} with 36002 Pa compared to the shaft with the same reinforcement size (R1=R2) and based on the filet variation from r = 3.75 to 22.5, turned out to be the best in reducing stress concentration at r = 5.625 or r/d = 0.075. This approach can optimize the shaft to reduce stress concentrations. The results are encouraging as the approach can lead to shaft optimization featuring multiple stress relief methods or experiencing multi-axial loads. Further development and application of this methodology to practical design cases should include appropriate safety factors.

REFERENCES

[1] W. Lin and T. Yoda, *Bridge engineering: classification, design loading and analysis method,* Butterworth-Heinemann, Elsevier Inc Press, 2017.

[2] W. D. Pilkey, D. F Pilkey, and Z. Bi, *Petersons's stress concentration factors*, USA: John Wiley and Sons, 2020.

[3] P. Taraphdar, R. Kumar, A. Giri, C. Pandey, M. Mahapatra and K. Sridhar, "Residual stress distribution in thick double-V butt welds with varying groove configuration, restraints and mechanical tensioning", *Journal of Manufacturing Processes*, vol. 68, pp. 1405-1417, 2021, doi: 10.1016/j.jmapro.2021.06.046

[4] V. A. Ermishkin, S. P. Kulagin, N. A. Minina, M. A. Pokrasin, "Determination of stress concentration factors from photometric analysis data", in *Journal of Physics: Proceeding of New Material and Technologies, XV IRCS,* Moscow, Russia, 2019, vol. 1347, doi: 10.1088/1742-6596/1347/1/012108

[5] T. I. Maulana, B. Soebandono, and A. Susanti, "Stress and deformation study on castellated steel beam with tapered shape and hexagonal openings," *SINERGI*, vol. 23, no. 1, pp. 61-69, 2019, doi: 10.22441/sinergi.2019.1.009

[6] X. Liang, J. Sheng and K. Wang, "Investigation of the mechanical properties of steel plates with artificial pitting and the effects of mutual pitting on the stress concentration factor", *Results in Physics*, vol. 14, p. 102520, 2019, doi: 10.1016/j.rinp.2019.102520

[7] M. Ozkan and I. Toktas, "Determination of the stress concentration factor (Kt) in a rectangular plate with a hole under tensile stress using different methods", *Materials Testing*, vol. 58, no. 10, pp. 839-847, 2016, doi: 10.3139/120.110933

[8] R. Norton, *Machine design: an integrated approach: Sixth Edition*, New Jersey: Pearson, 2020

[9] K. Vučković, I. Čular, R. Mašović, I. Galić and D. Žeželj, "Numerical model for bending fatigue life estimation of carburized spur gears with consideration of the adjacent tooth effect", *International Journal of Fatigue*, vol. 153, p. 106515, 2021, doi: 10.1016/j.ijfatigue.2021.106515

[10] M. Senthil Kumar, M. Santhosh, E. Arvind, M. Ashwin and S. Prashant, "Optimization of Spur Gear Design to Reduce Stress", *Applied Mechanics and Materials*, vol. 867, pp. 220-227, 2017, doi: 10.4028/www.scientific.net/AMM.867.220

[11] S. Sutar, G. Kumar and M. Doddamani, "Gear stress reduction using stress relief features:

A review", *Materials Today: Proceedings*, vol. 46, pp. 190-193, 2021, doi: 10.1016/j.matpr.2020.07.350
[12] F. Beer, E.R. Johnston, J. T. DeWolf, D.F. Mazurek, *Statics and mechanics of materials*, 3rd Edition. New York, NY: McGraw-Hill, 2021.
[13] M. Cicciù, G. Cervino, D. Milone and G. Risitano, "FEM Investigation of the Stress Distribution over Mandibular Bone Due to Screwed Overdenture Positioned on Dental Implants", *Materials*, vol. 11, no. 9, p. 1512, 2018, doi: 10.3390/ma11091512
[14] S. O. Effiom, F. Adam, B. Saeed, J. Evareh," Computational Design and Static-structural Analysis of a Small-scale Turbojet Propulsive Engine for an Unmanned Aerial Vehicle", *Nigerian Journal of Technology Research*, vol. 2, no, 1, pp. 1-7, 2020, doi: 10.4314/njtr.v16i1.5
[15] M. Ashby, "Material property data for engineering materials", 4th Edition, *Cambridge University*, Engineering Department and Granta Design, 2016
[16] D. Erena, J. Vázquez, C. Navarro and R. Talemi, "Numerical study on the influence of artificial internal stress relief groove on fretting fatigue in a shrink-fitted assembly", *Tribology International*, vol. 151, p. 106443, 2020, doi: 10.1016/j.triboint.2020.106443
[17] I. Onyegiri and M. Kashtalyan, "Threaded connectors for sandwich pipes – Part 2: Optimisation of stress relief groove", *International Journal of Pressure Vessels and Piping*, vol. 168, pp. 125-131, 2018, doi: 10.1016/j.ijpvp.2018.09.011
[18] D. Zeng, Y. Zhang, L. Lu, L. Zou, and S. Zhu. "Fretting wear and fatigue in press-fitted railway axle: A simulation study of the influence of stress relief groove", *International Journal of Fatigue*, vol. 118, pp. 225-236, doi: 10.1016/j.ijfatigue.2018.09.008
[19] J. Martínez, L. Vanegas Useche and M. Wahab, "Numerical prediction of fretting fatigue crack trajectory in a railway axle using XFEM", *International Journal of Fatigue*, vol. 100, pp. 32-49, 2017, doi: 10.1016/j.ijfatigue.2017.03.009
[20] M. Ozkan and F. Erdemir, "Determination of theoretical stress concentration factor for circular/elliptical holes with reinforcement using analytical, finite element method and artificial neural network techniques", *Neural Computing and Applications*, vol. 33, no. 19, pp. 12641-12659, 2021, doi: 10.1007/s00521-021-05914-x
[21] S. Mantovani, A. Chiari, M. Giacalone and A. Strozzi, "Shafts with U-shaped circumferential grooves: design charts for stress concentration factors, radial displacement and Poisson's ratio influence", *Proceedings of the Institution of Mechanical Engineers, Part C: Journal of Mechanical Engineering Science*, vol. 236, no. 16, pp. 9200-9217, 2022, doi: 10.1177/09544062221093910
[22] C. Wang, J. Wu, J. Cheng, S. Zhang and K. Zhang, "Elasto-hydrodynamic lubrication of the journal bearing system with a relief groove in the scroll compressor: Simulation and experiment", *Tribology International*, vol. 165, p. 107252, 2022, doi: 10.1016/j.triboint.2021.107252
[23] Y. Ma, Q. Wang, Z. Guo, G. Wang, L. Wang and J. Zhang, "Static and Fatigue Behavior Investigation of Artificial Notched Steel Reinforcement", *Materials*, vol. 10, no. 5, p. 532, 2017, doi: 10.3390/ma10050532
[24] H. Zeng, R. Yan, P. Du, M. Zhang and F. Peng, "Notch wear prediction model in high speed milling of AerMet100 steel with bull-nose tool considering the influence of stress concentration", *Wear*, vol. 408-409, pp. 228-237, 2018, doi: 10.1016/j.wear.2018.05.024
[25] D. Liao, S. Zhu, J. Correia, A. De Jesus and F. Berto, "Recent advances on notch effects in metal fatigue: A review", *Fatigue & Fracture of Engineering Materials & Structures*, vol. 43, no. 4, pp. 637-659, 2020, doi: 10.1111/ffe.13195
[26] Y. P. Asmara, "Simulation of CO2 Corrosion of Carbon Steel in High Pressure and High Temperature Environment (HPHT)," *Journal of Integrated and Advanced Engineering (JIAE)*, vol. 2, no. 1, pp. 63-70, 2022, doi: 10.51662/jiae.v2i1.41